Article Type: Contact Mechanics 2018 Special Issue

Corresponding Author Info: Andy Vickerstaff**,** Transport for London, Palestra, 197 Blackfriars Road, Southwark, London, SE1 8NJ, UK E-mail: AndyVickerstaff@tfl.gov.uk

Article title: PREDICTIVE WHEEL-RAIL MANAGEMENT IN LONDON UNDERGROUND: VALIDATION AND VERIFICATION

Authors: Andy Vickerstaff**,** Transport for London, Palestra, 197 Blackfriars Road, Southwark, London, SE1 8NJ, UK

Adam Bevan, Institute of Railway Research, University of Huddersfield, Queensgate, Huddersfield, HD1 3DH

Pelin Boyacioglu, Institute of Railway Research, University of Huddersfield, Queensgate, Huddersfield, HD1 3DH

Abstract

London Underground is facing the challenge of increasing timetables against spending cuts across renewals and maintenance in all assets. In order to meet this challenge, it is reviewing all maintenance practices to make sure they are appropriate for current asset conditions. Management of the wheel-rail interface is critical to maximising the life of wheels and rails through preventative maintenance regimes that ensure all activities offer value for money and safe operation.

Detailed monitoring of asset condition using novel non-destructive techniques has allowed the identification of the problems which currently occur at the wheel-rail interface on the LUL network. These problems are discussed in this paper along with some of the solutions proposed to manage them.

Site observations from a range of rail rolling contact fatigue (RCF) monitoring sites have also been compared to the outputs from vehicle dynamic simulations. These outputs were post-processed using a circle plotting technique, which illustrates the location, direction and severity of the forces, and the Whole Life Rail Model (WLRM) to predict the susceptibility to rail damage for two rail steel grades. The outputs from these comparisons have helped to illustrate the wheel-rail contact conditions and forces which are driving the observed damage and potential future enhancements to improve the accuracy of the models for predicting the observed RCF damage.

Keywords: Wheel profile management, rail profile management, rolling contact fatigue, adhesion management, preventative maintenance.

1. Introduction

Management of the wheel-rail interface (WRI) on London Underground (LUL) has been at best sporadic throughout its history. The level of attention paid to it has often been driven by the political landscape of the day and reactions to major failures of the interface[1]. Since December 2017, the final vestiges of the Public Private Partnership (PPP) have been removed and for the first time since December 2002, LUL has been re-organised into one business with single points of accountability for Track and Rolling Stock.

To examine the problems in both wheels and rails, a WRI team was established in 2012. Major improvements have been delivered since then including implementation of preventative maintenance regimes for wheel re-profiling and a rail grinding regime for sites which are highly susceptible to rolling contact fatigue (RCF) cracking [2,3]. However, against a backdrop of increasing tonnages and reduction in spending, it is even more imperative to quantify the benefits of all maintenance activities. A key element of this strategy is the ability to accurately predict when wheels and rails will fail and implement appropriate preventative maintenance activities.

This paper presents the problems which occur at the WRI on the LUL network and discusses the current solutions proposed to manage them. The outputs from vehicle dynamics simulations are presented to illustrate the wheel-rail contact conditions and forces which are driving the observed damage. These outputs have been post-processed using a circle plotting technique[4], which provides an indication of the location, direction and severity of the forces, along with the Whole Life Rail Model (WLRM)[5]. The susceptibility to rail damage for two rail steel grades (e.g. R260 and HP335) have been compared to site observations for a range of RCF monitoring sites on the LUL network.

2. Wheel Profile Management

LUL consists of a number of different lines, each with their own dedicated fleet of rolling stock which have historically managed their wheelsets in different ways. The majority of fleets operated a 'run to fail' policy through the use of maintenance and 'go/no-go' gauges. These gauges are used to identify when wheels are approaching flange height, thickness and hollowing limits, but if they still pass the 'go/no-go' gauge, then they could be returned to service with wheel turning planned in before the next inspection. Even though the 'run to fail' policy was suitable when operating a limited service with spare train capacity, increases in timetables means that more trains are required to operate the enhanced service and hence, unscheduled maintenance must be avoided. A planned preventative wheel re-profiling regime was required to ensure a sufficient number

of trains are available for service which comply with the relevant standards. This also allows for wheel lathe demand to be accurately managed to ensure that demand does not exceed capacity.

In order to achieve this a wheel profile monitoring programme was introduced to establish the principal mode of failure and the rate of degradation across each individual fleet so that a preventative wheel turning interval could be implemented within each Train Maintenance Regime (TMR). The wheels were measured using the MiniProf™ device and each fleet's Minimum Action Codes (MAC) for wheel defects were also reviewed. It was clear from the analysis of each fleets MAC that they had been written based on their particular failure mode rather than representing the severity of the defect and its potential risk. The output from this review resulted in consistency across all fleets in how defects were treated and recorded.

The majority of LUL stocks operate using an LT5 wheel profile, whilst a number of legacy fleets still operate with the former LT3 profile. Figure 1 displays the rolling radius difference (RRD) generated with both new and worn LT5 and LT3 wheel profiles on a new and worn 56E1 rail sections. The rolling radius difference (RRD) is important for understanding the potential steering performance of the different wheel and rail profile combinations. Although, both of the profiles have a cone angle of 1 in 20, the LT5 has a more gradual change in radius where the tread meets the flange angle. This results in a more gradual change in RRD which generates a greater steering force for a smaller lateral shift of the wheelset. In addition, a greater lateral shift of the wheelset is required to produce flange contact as illustrated in Figure 1. As demonstrated using vehicle dynamics simulations, this means that flange contact does not typically occur until approximately 600 m radius curve for LT5 compared to 1000 m radius for LT3. As the profiles wear the LT3 profile generates a high conicity, whilst the LT5 generates a lower or negative conicity due to hollow wear as described below.

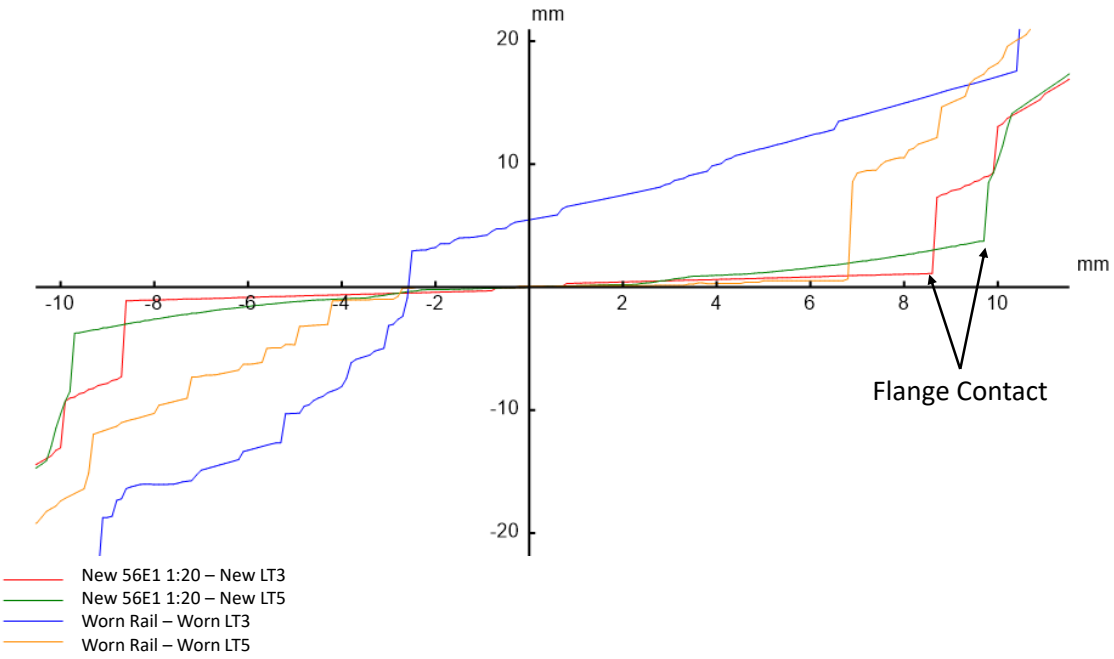

Figure 1: Rolling radius difference generated between new and worn LT5 and LT3 wheels

The rolling stock, wheel profiles and turning intervals differ for each line and fleet. Initially, the intervals were determined in kilometres travelled since last turn however, this was converted to a time-based interval on some legacy fleets. But, care must be taken when defining a time-based interval for routine maintenance as the train path can vary by as much as 400 km from one day to another. Also, the fleet characteristics can influence the turning regime. For example, due to the different braking systems and resulting wear patterns on the motor and trailer wheelsets of the 2009 tube stock (09TS), which operates on the Victoria line, different turning intervals were recommended.

Assessment of the measured profiles showed that the failure mode for LT3 wheel profiles is predominantly through reaching flange height or width limits, with the coning angle being retained throughout the lifecycle as can be seen in Figure 2(a). There was also signs of tread rollover and visual RCF in the flange root, but these were usually within safety limits when wheels are turned.

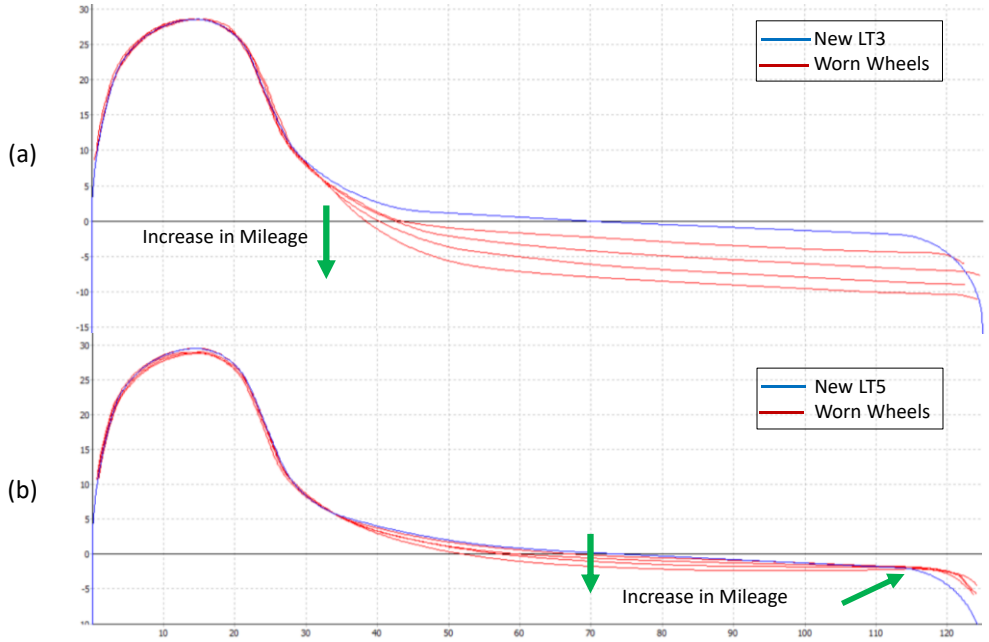

Figure 2: Failure mode of (a) LT3 and (b) LT5 wheel profiles

In comparison, the LT5 profile as illustrated in Figure 2(b) primarily fails through a combination of wheel hollowing and tread rollover. The RRD generated by wheel profiles with high levels of hollowness will result in a negative slope and therefore a low or negative conicity. This will prevent the wheelset from steering towards an optimal rolling position, resulting in higher wheelset angles of attack and increased wheel-rail forces. A hollow wear limit of 2 mm has been defined, since this is the point at which all the conicity is reduced to zero and hence, the wheel is no longer capable of generating any steering force.

The analysis of in -service wheel profiles and tread surface condition has helped to identify the main drivers for wheel maintenance and recommendation of appropriate maintenance intervals. It also supports the modelling through a better understanding of the distribution of worn wheel profiles, and therefore contact condition, currently in operation on the network.

3. Rail Defect Management

Previously broken rails was a significant problem on LUL, however the number of broken rails has reduced significantly in the last 20 years owing to implementation of comprehensive track renewal programme and the use of advanced non-destructive testing (NDT) techniques, such as B-Scan ultrasonic testing, to detect railhead defects.

Figure 3 displays the number of broken rails per year since 2011 for each of the operating lines on LUL. As it can be seen, the major increase occurred in the 2013/2014 was reduced in the following years. The Piccadilly (PIC) and Northern (NOR) lines are suffering from the highest number of broken rails which stems from the larger

proportion of jointed bullhead rail in plain line, where approximately 37% of rails are bullhead. Further analysis of the rail type for each break highlights the greatest risk is with the remaining bullhead rail on the network as approximately 90% of rail breaks occur in bullhead rail. Since the mid-1980s track replacement projects have moved to replacing bullhead with flat bottom rail, with an approximate proportion of rail type of 60% flat bottom to 40% bullhead currently across the network. Therefore the distribution of bullhead rail will generally be older than flat bottom rail, potentially increasing the risk of rail breaks. However asset management systems are not sophisticated enough to allow an actual date of installation to be ascertained so, with the exception of monitoring sites, determining the precise rail age and whether rail breaks occur in newer or older rails is difficult.

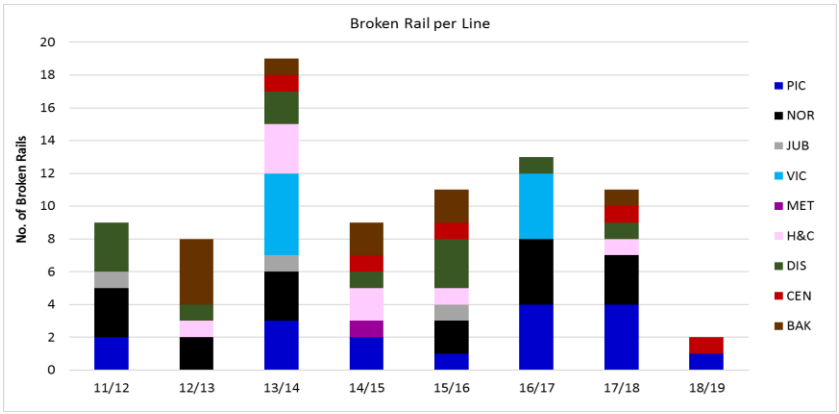

Figure 3: Number of broken rails on each LUL line per year (from 2011 to July 2018)

Since 2012, the breaks which have occurred in flat bottom rails have generally been related to a defective batch of flashbutt welds, alumino-thermic welds which have had gross porosity or rail foot corrosion. These type of defects are currently either extremely difficult or impossible to detect ultrasonically.

The most common failure leading to bullhead broken rails relates to fishplate fretting due to movement of rails at the joint edge where the plate rubs against the rail foot and causes a stress raiser from which cracks can be generated. These then propagate to bolt holes, up through the top surface causing a full fracture. The initiation of this type of defect from the external web of the rail is untestable by ultrasonics until the crack reaches the centre of the rail by which time it is often too late and fast fracture has already occurred. Therefore, prevention of this type of defect is solely reliant on visual inspection lighting, however introduction of better torque wrenches and instructions to tighten joints specifically has helped to reduce the occurrence.

The frequency of rail defects in plain line track, detected in the rail head using visual and ultrasonic NDT, have been seen to gradually reduce since 2013 despite an increase in tonnage, as presented in Figure 4 for each of

the operating lines. However, an increase in 2017/18 was observed due to the trialling of a grinding method which did not remove sufficient material from the railhead to prevent damage re-occurring.

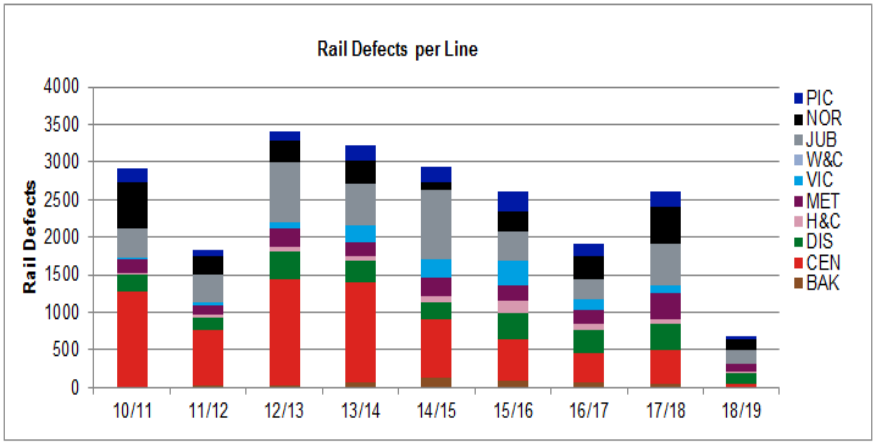

Figure 4: Frequency of rail defects in plain line track since 2010

The most frequently occurring defect on the network is the so called squat type defect[6]. These mostly occur in open sections, where adhesion conditions can be low enough to cause wheel slide protection (WSP) activation, which is reflected in the larger proportion on the Jubilee (JUB), Northern (NOR) and Central (CEN) lines. It is also noticed that they mostly generate at locations where trains have to stop regularly and drivers apply earlier braking at a lower rate to adjust for low adhesion conditions.

3.1 Monitoring of RCF Defects

Historically on LUL, the dominant damage mechanism was wear rather than RCF due to higher percentage of tighter curves and lesser control over lubrication. The introduction of newer trains and the increasing cost of replacement works, a greater focus was placed on combating and managing rail wear, resulting in greater susceptibility to RCF. Therefore, to effectively manage this problem, particularly the interaction between wear and RCF, higher emphasis was placed on introducing preventative maintenance regimes such as rail grinding in order to reduce failures. In order to optimise the rail grinding interval, it is important to understand the depth of the RCF cracking into the rail which indicates the level of maintenance required to rectify the defect.

LUL have recently introduced the Rail Surface Crack Measurement (RSCM) system manufactured by MRX Technologies, which measures the depth of RCF through magnetic flux leakage up to maximum 7 mm into the railhead[7]. Previously, RCF monitoring was primarily based on surface crack length which is incredibly labour intensive requiring precise visual inspection and detailed data recording. The use of this monitoring tool resulted in a revision to re-railing requirement to ≥ 5 mm crack depth, as the cracks deeper than this limit cannot be removed by grinding which in turn resulted an approximately 20 km of re-railing work across the network.

4. Rail RCF Modelling

To support the development of future maintenance plans accurate rail damage models are required to predict the locations susceptible to damage, estimate the growth rates and potential material removal through grinding at these locations prior to next inspection. Detailed Vampire™ vehicle dynamics route simulations of the entire network have been carried out in order to predict the changes in wheel-rail forces and ascertain realistic performance expectations of the wheel-rail interface. These simulations have also helped to calculate the main input parameters of some of the RCF damage prediction models.

One of the commonly used damage models is the Whole Life Rail Model (WLRM). This model includes a damage function (see Figure 8) which describes interaction of RCF and wear to predict the susceptibility of a rail steel to crack initiation based on the contact patch energy (Tγ)[5]. It has been largely implemented and validated in real-case studies and provides an opportunity to investigate how different vehicle-track characteristics affect RCF susceptibility by integrating vehicle dynamics simulation outputs in its model framework[8]. Other commonly used models are based on Shakedown theory, which uses the contact stress and traction coefficient parameters to predict the rail's propensity to damage[9]. Based on the area within the Shakedown map, different type of failure mechanisms are predicted such as high and low cycle fatigue[10,11] and ratchetting. A number of models have been developed which utilise the Shakedown map, including the Surface Fatigue Index (FI_{surf})[12], in which the rate of crack initiation increases as the load increases. Several studies[13,14] have been undertaken to compare the outputs from FI_{surf} and the WLRM and the Stress Index (SI) and Energy Index (EI) were subsequently developed to improve the prediction accuracy of the model by incorporating the longitudinal and lateral shear stresses[15].

Even though the WLRM has mainly been applied on GB mainlines, its performance on routes with different characteristics is generally unknown. Thereby, to test its applicability on metro systems, an initial study to investigate rail damage mechanisms on LUL was conducted[16]. The influence of key factors such as curve radius, wheel-rail friction conditions, track irregularity levels and wheel-rail profiles on the predicted Tγ were examined for the Bakerloo (LT3 wheel) and Jubilee (LT5 wheel) lines and compared with a GB mainline route (Midland Mainline, P8 wheel). It was found that the Tγ can successfully show the changes in the susceptibility to rail damage under various vehicle-track characteristics and between different lines. For example, while the smaller curve radius located on metro lines increases the level of Tγ, the application of lubrication reduces the friction coefficient at the wheel-rail interface which in turn reduces the level of Tγ potentially resulting a higher RCF than wear damage risk. The Tγ values were also shown to vary between the two LUL lines studied, with the higher

additional traction forces and the LT3 profile on the Bakerloo lines generating a substantial increase in the Tγ levels. This showed that all the vehicle-track characteristics as well as the wheel-rail profile pairs play an important role in the resulting Tγ and therefore rail damage.

It should be highlighted that the Tγ in the WLRM is the 'signed Tγ' which assumes that the creep forces in the traction direction will cause damage to the rail, whereas forces in the braking direction will generate RCF on the wheel[17]. However, some of the previous results demonstrated that the damage can vary according to the angle of the resultant creep force, rather than in the traction direction only[18,19]. Therefore, to present the changes in creep force angles and to illustrate a more clear comparison between LT5 and LT3 wheels, the circle plots are presented in Figure 6. These plots, as illustrated in Figure 5, allow interpretation of the contact position on the rail (indicated by the radial y position, with the gauge face in the middle of the circle) and the direction of the creep forces (represented by angular position around the circular plot, with Ψ = 0° represents the braking direction and Ψ = 180° represents the traction direction). The magnitude of the force or damage is also indicated by the colour of the spots, where in this case the colour of the spots represents the magnitude of the predicted T_γ (with red representing the peak of the WLRM damage function, Figure 8).

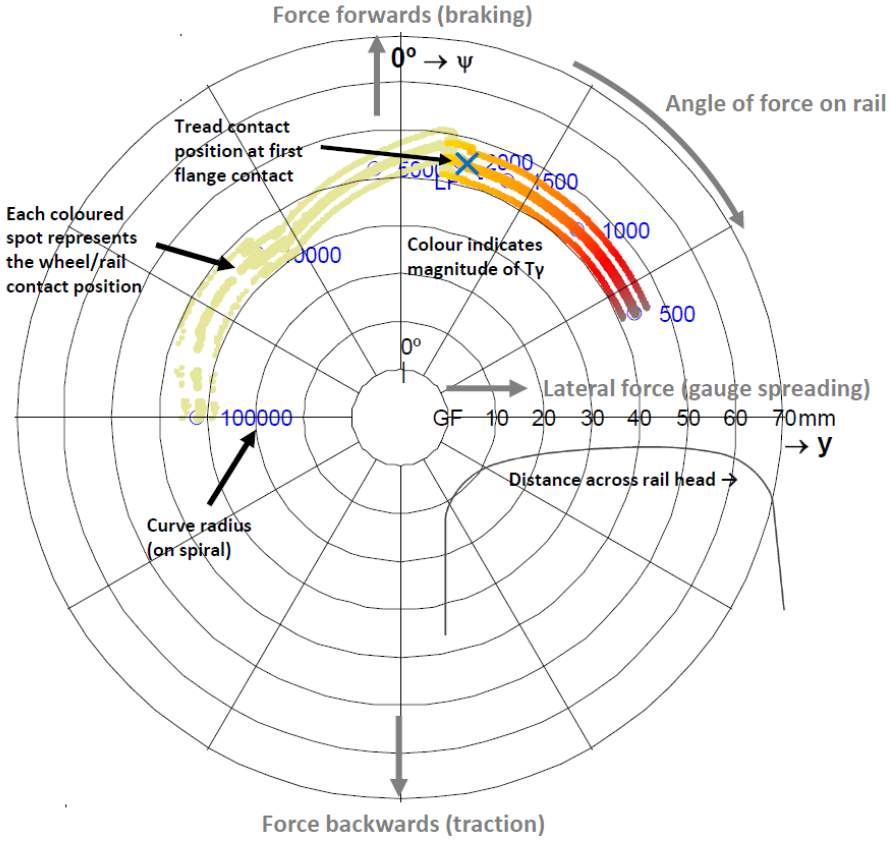

Figure 5: Interpretation of the circle plots

The circle plots presented in Figure 6 display for the contacts generated at the leading (top) and trailing (bottom) axles on the high rail as a result of generic simulations which consist of a range of curve radii (reducing from 4000 m to 50 m) with a model of the S-stock vehicle operating with the LT3 and LT5 wheel profile.

As it may be expected from the RRD comparison plot (Figure 1), the lower conicity in the LT3 wheel results in two-point (tread and flange) contacts, which can be seen by the two distinct contact bands at approximately y = 5 mm and y = 30 mm, with relatively large Tγ values. Also, the curve radii indicated by black (flange) and blue (tread) coloured labels demonstrate that two-point contact occurs under 1000 m radius curve. In contrast, the shape of the higher conicity LT5 wheel profile tends to generate a more conformal single-point (either tread or flange) contact, with the Tγ levels increasing as the contact approaches the wheel flange / rail gauge corner. For example, the black coloured '200 m' represents the single flange contact on that curve radius. Under both wheel profiles, the wheel-rail contacts generated at the trailing axle seem to provide a higher RCF risk (indicated by a large volume to red spots) in the centre of the rail crown (30 mm < y < 40 mm) even though the forces appear to be in the braking 'non-damaging' direction, while the leading axle gives rise to higher wear risk (indicated by a larger volume of green spots, Tγ ≥ 175 N) close to the rail gauge corner (y < 10 mm). However, it is apparent that the damage risk reduces under the LT5 wheel.

As previously discussed, the original development of the WLRM focused on the prediction of classic high rail gauge corner RCF seen on GB mainline curves where the assumption that damage is only caused by creep forces in the traction direction is valid. However, it is possible that the forces generated by the trailing axle under the conditions found on the LUL network could contribute to other forms of rail damage for which the original WLRM was not developed to predict. This is further investigated below through comparison with site observations.

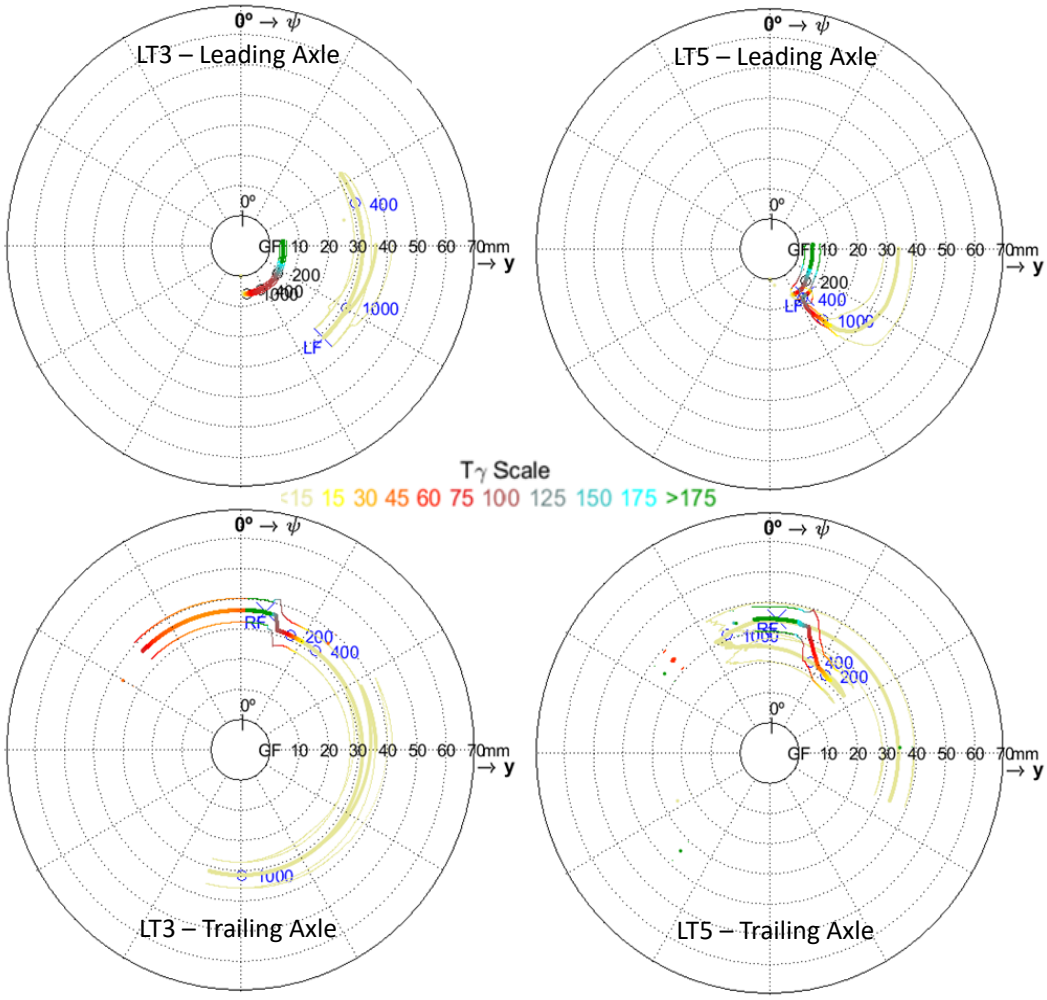

Figure 6: Circle plot comparing the location, direction (angle) and magnitude (Tγ) of the creep forces generated on the high rail when operating on a range of curve radii with LT3 (left) and LT5 (right) wheel profiles

To increase the efficiency in visual inspections, magnetic particle inspection (MPI) is also used and the photographs are taken accordingly. This helps to detect the surface and near-surface flaws in ferromagnetic particles, enabling cracking to be observed more easily[20]. Figure 7 displays the photos under MPI from a 400 m (left) and 200 m (right) radius curve which are operated with rolling stock consisting of the LT5 wheel profile. It can be seen that they show good agreement with the creep forces presented in the LT5 circle plot. On a 400 m radius curve, the leading axle with an LT5 wheel profile generates a single RCF band (as highlighted by the green box) towards the gauge corner of the rail. On a 200 m radius curve, the leading axle gives rise to wear (as highlighted by the blue box) with a small band of RCF cracking (as highlighted by the orange box), whilst the forces generated by the trailing axle seem to be responsible for the similar RCF band (as highlighted by the green box) towards the centre of the rail crown. It is also worth noting that the direction of the forces at these locations

are perpendicular to the observed angle of cracking, suggesting that a change to the assumptions within the original WLRM could be required in order to predict this band of damage

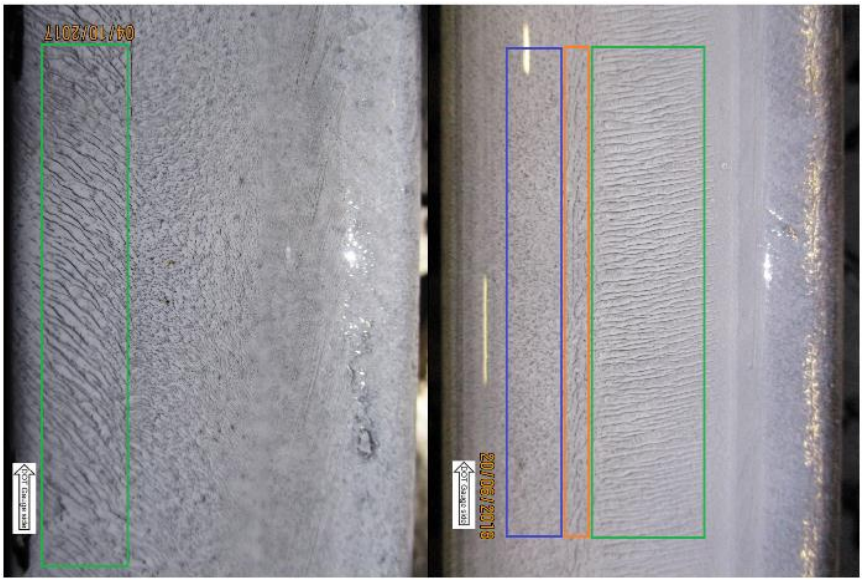

Figure 7: Comparison of RCF observations on high rails of the 400 m (left) and 200 m (right) curves

4.1 Comparison of Model Predictions with Site observations

To optimise the maintenance planning and to support the modelling studies, it is important to observe the crack development (e.g. initiation and propagation) on site. LUL have recently introduced an intensive monitoring campaign for re-railed sites where RCF was frequently reported in the past. Approximately 60 sites have been included in this study which covers different rolling stock, a variety of rail types and curve radii between 70 and 1000 m. The rail condition at these sites has been monitored at certain intervals using several measurement techniques, including MRX-RSCM and MiniProf profile measurements, to detect the severity of any defects and level of rail wear. In addition, the rail surfaces have been also photographed under MPI to improve the visibility of the cracks. Besides their use in RCF monitoring, this data also provides valuable input for the vehicle dynamics simulations and an opportunity to validate the damage predictions.

In an attempt to increase the rail life apparent under R260 steel grade, some of the high rail sites have been replaced with the high performance rail steel HP335 steel[21]. Grade HP335 is a naturally cooled hypereutectoid steel from British Steel that has been approved and successfully deployed by Network Rail, but it is not yet included in EN13674-1 2011[22]. To evaluate the performance of the different rail steels, the WLRM damage function for R260 and HP335 rail steels were used. The differences in these damage functions are presented in Figure 8 and were developed based on site observations, differences in material properties and their performance during twin disc testing[18]. Although the validation of this new function for HP335 is still ongoing, a

recent study which compared the outputs from vehicle dynamics simulations with field observations for R260Mn and R370CrHT rail steel grades also found that increasing the fatigue crack initiation limit and a reduced slope of the peak RCF damage line provided better correlation with the crack appearance on the R370CrHT rail surface. Based on the proposed damage function, it may be expected that HP335 rail will also experience a slower rate of RCF initiation with reduced wear risk, as it requires higher energy levels compared to R260 damage function. This also means that where wear may dominate (with $T\gamma > 175$ N) under R260 rail, the RCF risk is still increasing (up to $T\gamma \leq 235$ N) under HP335 rail.

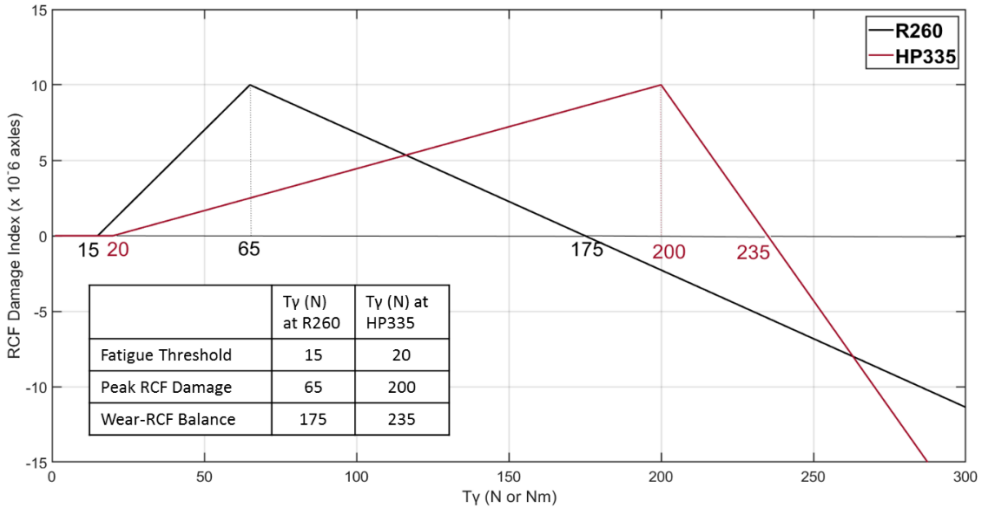

Figure 8: WLRM for R260 and HP335 rails[18]

To have an initial assessment of the rails' performance with R260 and HP335, the WLRM damage index was predicted using a vehicle model of1992 tube stock (92TS) and are plotted against curve radius in Figure 9. As expected, the HP335 rail causes a reduction in RCF damage susceptibility when operating with both the LT3 and LT5 wheel profiles on curves with radii > 200 m. For example, the estimated RCF risk decreases by 65% on a 500 m radius curve with the LT3 wheel, indicating that the crack initiation may generate at a slower rate compared to a normal grade rail. In general, the decrease in curve radius leads to an increase in the rails susceptibility to damage. However, while the peak RCF damage is predicted to occur at a curve radius of ≈ 600 m, the rate of rail wear also starts to dominate as the curve radius reduces on grade R260 rail steel. On the other hand, the RCF risk for HP335 reaches its peak at ≈ 120 m radius curve, again when wear becomes the dominant damage mechanism on very sharp curves (R<120 m). Between the curvature range 200 m > R > 120 m, it is also apparent that the HP355 may cause higher RCF risk compared to R260 steel grade. When two wheel profiles are compared, it can be seen that the LT5 wheel causes slightly higher RCF risk at

≈ 285 m radius curve, where the LT3 wheel profile is predicted to generate greater wear, removing the RCF cracking in this curve range. However, as displayed in Figures 1 and 6, it should be noted that the different profile shape and conicity levels of these two profiles result in different contact conditions and the resulting location of the damage on the rail head will be different as indicated in the circle plots.

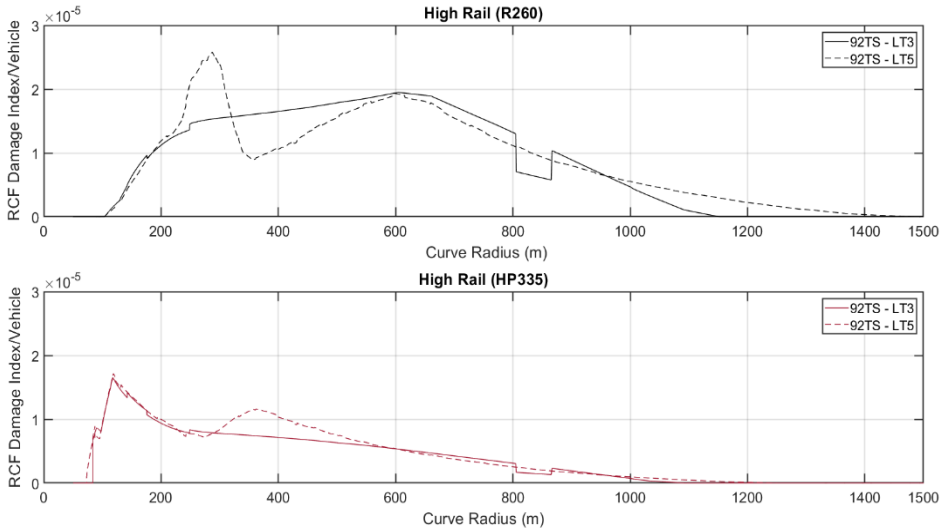

Figure 9: Comparison of RCF Damage Index for both of the wheels under R260 and HP335 models

Figure 10 displays the differences in RCF observations between the two rail steels on curves with the same radii (R = 400 m). Even though the sites are located on different lines with variations in worn wheel profiles, the lower RCF risk predicted by WLRM on HP355 rail is evident, with the initiated cracking following 13 million gross tonnes (MGT) becoming more severe as tonnage increases on the normal grade rail.

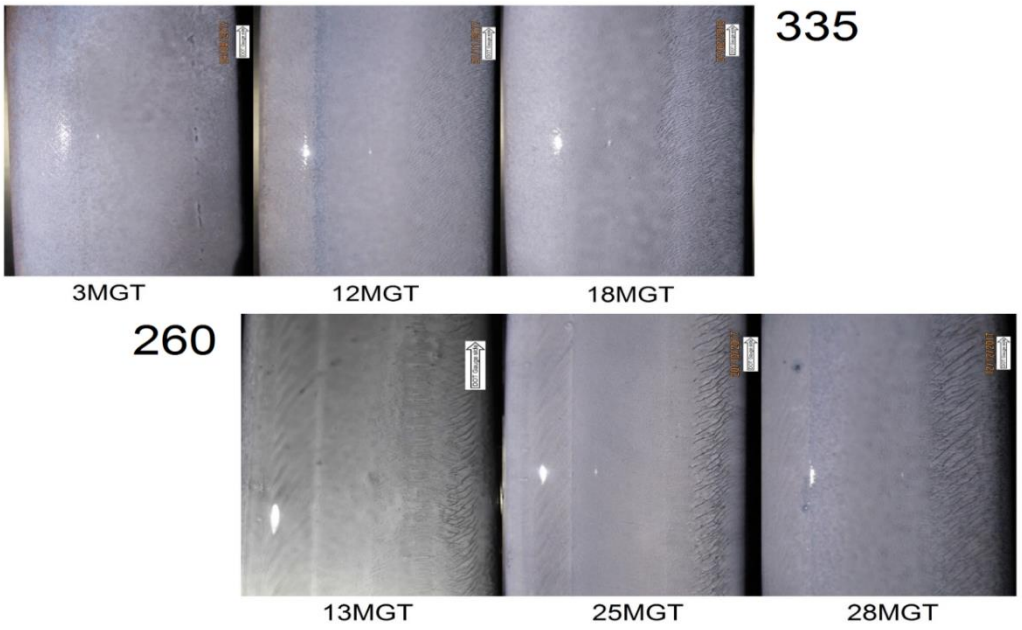

Figure 10: Differences in RCF observations between R260 and HP335 rails under similar R=400 m curve

In order to provide a more detailed comparison, the circle plots are compared with the site photographs. One of the historically RCF-prone sites is located on the Central Line (Caxton curve, RCF-CEN-7) and consists of 70 m radius left-hand curve. It was recently re-railed with HP335 due to severe cracking. Figure 11 displays the location, direction and severity of the predicted Tγ, with red colour indicating the peak of the proposed HP335 damage function.

Due to the presence of a check rail at the site, no gauge corner contact (y < 30 mm) is predicted on the high (left) rail. Therefore, wear mainly occurs on the crown of the rail due to both the leading and trailing axles. The location and severity of the predicted forces suggests that RCF is again mainly driven by the trailing axle, with high levels of peak RCF damage (orange and red spots) in the longitudinal direction providing a good indication of a high susceptibility to horizontal cracking on the rail head. Nevertheless, the low RCF damage (yellow spots with 20 N > Tγ > 50 N) generated under the leading axle may seem to give rise to plastic flow.

On the low (right) rail, the Tγ on the leading axle is mainly in the wear region of the damage function, potentially resulting in the rail crown flattening observed on site (green spots with Tγ > 235 N). In comparison, the trailing axle generates damaging Tγ levels (orange-red spots,) close to gauge corner of the rail. These suggest a high susceptibility to low rail gauge corner cracking which has been observed on site.

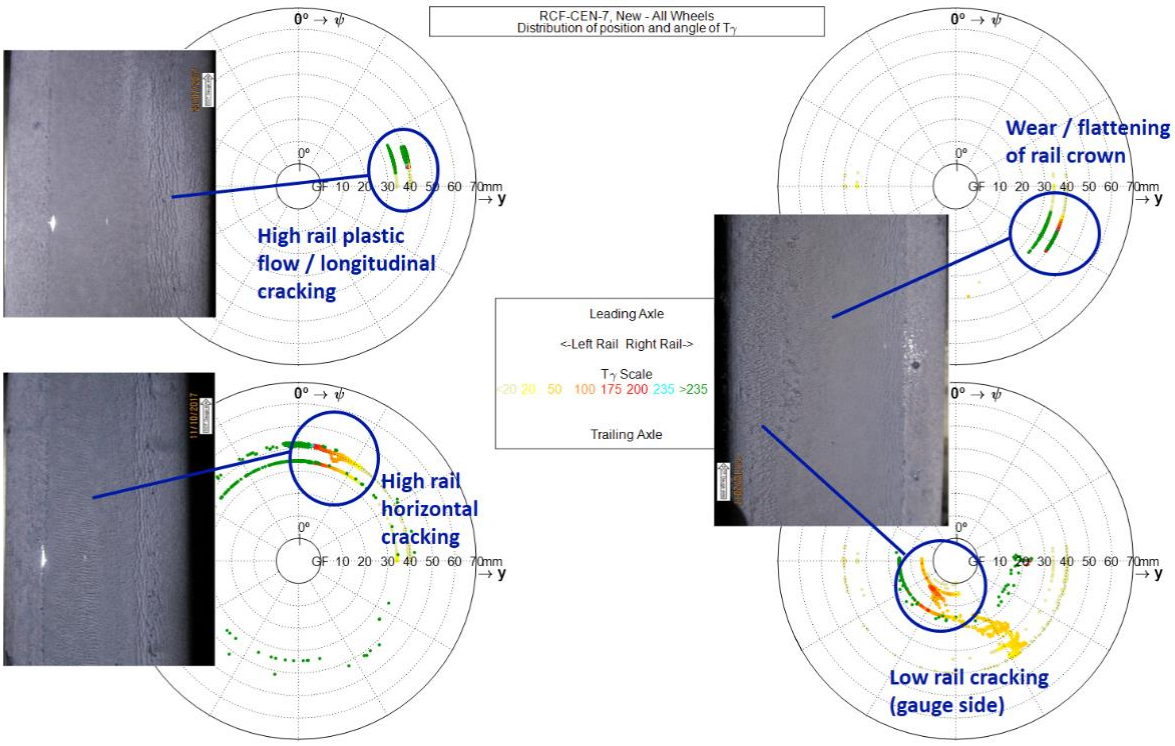

Figure 11: Circle plots for RCF-CEN-7 and comparison with site observations

Correlation of the predicted wheel-rail forces with the site observations suggests that the transverse defects observed at a number of sites on LUL appear to be mainly driven by forces in the braking direction generated by the trailing axle. As previously discussed; in the original application of the WLRM forces in the braking direction would be scaled to zero (e.g. non-damaging), as forces in this direction are not associated with classic high-rail RCF for which the WLRM was originally developed to predict. Thus, an alternative scaling method is required to predict this damage on LUL.

In addition, the RCF crack depth with its growth rate should be accurately predicted to develop a preventative rail grinding regime. This will allow the estimation of the depth of material required to be removed from the railhead to remove the predicted damage based on the time period since the last grinding activity. Future grinding intervals can then be determined and a more detailed cost/benefit analysis can be carried out.

Further research is being undertaken at the University of Huddersfield's Institute of Railway Research (IRR) to increase the accuracy of damage predictions in order to aid future maintenance planning optimisation on metro systems[16,23]. A significant volume of vehicle-track data has been analysed, including RCF crack depth measurements (using MRX-RSCM), MiniProf wheel and rail profiles measurements, track geometry, traffic information and rail maintenance history. This data was used to build detailed vehicle dynamics simulations to help understand the key changes in contact parameters which influence the observed rail damage. As a result of this study, a combined Shakedown Map and Tγ approach is been investigated to predict the depth of RCF cracking.

5. Adhesion Management

Adhesion management across the LUL network is carried out through a combination of various types of track based lubricators as well as train borne 'stick' systems installed on a number of newer trains. Additionally, top of rail (TOR) protection is provided by track based units for specific sites and on-board system on a number of fleets.

As previously stated in Section 3.1, historically LUL have largely suffered from rail wear, especially on the sub-surface network. As tracks have been modernised to flat bottom rails, this brought increased costs and hence a higher proportion of the resources was dedicated to the installation of track lubricators in the early 2000s to combat wear. However, the reduction in rail wear makes RCF the dominant failure mode.

Through the introduction of new rolling stock a concerted effort has been made to reduce the number of track lubricators. This again makes vehicle dynamics simulations results essential to enable a more accurate prediction

of when flange contact occurs and where gauge corner lubrication is required. Although numerous factors affect the precise location of flange contact, it has been shown through simulation to start at approx. 600 m radius curve under the LT5 wheel profile, while the lower conicity of the LT3 wheel profile (Figure 1) results in an earlier initiation at approx. 1000 m radius curve. Based on this finding approximately 50 track lubricators have been removed on curves greater than the 600 m radius limit.

The overall adhesion management strategy for LUL is to provide as much protection on-board the vehicle as this is significantly easier to maintain, as sticks can be renewed as part of routine inspection/maintenance and removes the requirements for track access. However, the current on-board systems provide no protection to the back of the flange and hence, check rails will still require track based lubrication.

6. Conclusions

Understanding of the WRI on LUL has increased enormously in the last 6 years through a combination of: detailed data collection and analysis, introduction of modern technologies to more accurately monitor rail defects and vehicle dynamics modelling to more accurately predict failures.

Wheel turning is now a routine maintenance activity which can be planned accurately to ensure compliance to the standards and maintain conicity. As timetables continue to require more trains in service, a 'run to fail' regime is no longer a sufficient maintenance strategy. Accurate planning also enables wheel lathes to avoid routine turning during the autumn leaf fall season especially on lines vulnerable to wheel flats.

Rail RCF is now the dominant failure mode on LUL rather than wear and rail replacement is a far more costly activity than it was with legacy bullhead components. Thereby, preventative rail grinding is essential to avoiding emergency rail defects which results in service disruptions and expensive reactive maintenance. Rail grinding in engineering hours will always be far more expensive than operating in closures and the operational business will have to make difficult decisions in future, balancing cost and impact if efficiencies are to be realised. Rail monitoring techniques have vastly improved in recent years and allow the planning of maintenance interventions more accurately than before, but given the reduced access available and longer lead times to secure it, they are not yet accurate enough to solely rely on condition based measurements.

The application of the WLRM and circle plots show good agreement with the site observations and help to highlight the curves on the LUL network which are most at risk from RCF cracking. The comparison of the location, direction and severity of wheel-rail forces with site observations has identified the contacts which are more responsible for wear and RCF damage. While the leading axles tends to generate more wear, the trailing

axle was shown to give rise to transverse cracking particularly in tight radius curves. As some of these predicted forces are in the braking direction, this shows that an alternative scaling method within the WLRM is required to increase the accuracy of RCF predictions on LUL.

Comparisons of damage predictions has demonstrated that the HP335 rail steel can potentially result in a lower rate of RCF crack development which was also evident in observations from real track cases. It is also apparent that the interaction of wear decreases (particularly under sharper curves) and this may give rise to a higher RCF risk under certain conditions. However, further comparisons between site observations and damage predictions are required to validate the proposed WLRM damage function for HP335 rail steel.

Acknowledgments

The results presented within this paper have been collated by dedicated engineers that form the wheel-rail interface team alongside the first author and I would like to express my thanks to them for their continued efforts and expertise: Matthew Lee, Christine Baldwin and Dennis Johnston-Webber.

References

1. Baker P, Newton S. Wheel and Rail Wear on London Underground: The Problems and Solutions. In: 2nd Mini Conference on Contact Mechanics and Wear of Rail/Wheel Systems. Budapest, Hungary; 1996.
2. Vickerstaff A. Predict and Prevent:The future of wheelset management on London Underground. presented at the 21 Wheel-Rail Interaction Conference. 2015.
3. Vickerstaff A. A Holistic approach to WRI Management on London Underground. presented at the 22 Wheel-Rail Interaction Conference. 2016.
4. Molyneux-Berry P, Bevan A. Wheel surface damage: Relating the position and angle of forces to the observed damage patterns. Veh Syst Dyn. 2012;
5. Burstow MC. Whole Life Rail Model application and development: Development of a rolling contact fatigue damage parameter. Rail Safety and Standards Board. 2003.
6. Grassie SL, Fletcher DI, Hernandez EAG, Summers P. Studs: a squat-type defect in rails. Proc Inst Mech Eng Part F J Rail Rapid Transit. 2011;0954409711421462.
7. MRX. Rail Surface Crack Measurement Manual. 2011.
8. Burstow M, Fletcher DI, Franklin FJ, Kapoor A. Management and Understanding of Rolling Contact Fatigue:WP1 Mechanisms of Crack Initiation. 2008.
9. Johnson KL. Plastic deformation in rolling contact. Springer; 2000.
10. Franklin FJ, Chung T, Kapoor A. Ratcheting and fatigue-led wear in rail–wheel contact. Fatigue Fract Eng Mater Struct. 2003;26(10):949–55.
11. Ringsberg JW, Loo-Morrey M, Josefson BL, Kapoor A, Beynon JH. Prediction of fatigue crack initiation for rolling contact fatigue. Int J Fatigue. 2000;22(3):205–15.
12. Ekberg A, Åkesson B, Kabo E. Wheel/rail rolling contact fatigue–Probe, predict, prevent. Wear. 2014;314(1):2–12.
13. Stichel S, Mohr H, Ågren J, Enblom R. Investigation of the risk for rolling contact fatigue on wheels of different passenger trains. Veh Syst Dyn. 2008;46(1):317–27.
14. Dirks B, Enblom R, Skolan för teknikvetenskap, Kth, Spårfordon, Farkost och flyg. Prediction model for wheel profile wear and rolling contact fatigue. Wear. 2011;271(1):210–7.
15. Dirks B, Enblom R, Ekberg A, Berg M. The development of a crack propagation model for railway wheels and rails. Fatigue Fract Eng Mater Struct . 2015;38(12):1478–91.
16. Boyacioglu P, Bevan A&, Vickerstaff A. Prediction of RCF Damage on Underground Metro Lines. Am Soc Civ Eng. 2017;ICRT 2017:207–25.

17. Burstow M. Background to the Tγ RCF damage function . 2006.
18. Bevan A. Further Devolopment of the WLRM Damage Parameter . 2011.
19. Evans JR, Lee TKY, Hon CC. Optimising the wheel/rail interface on a modern urban rail system. Veh Syst Dyn. 2008;46(S1):119–27.
20. Lundh M. Automatic crack detection in forged metal parts-an image analysis approach. Chalmers University of Technology; 2012.
21. Carroll R, Smith HM, Jaiswal J. Rail Steel with an excellent combination of wear properties and rolling contact fatigue resistance. EP 2 247 764 B1.
22. BS EN 13674-1:2011+A1:2017: Railway applications. Track. Rail. Vignole railway rails 46 kg/m and above. British Standards Institute. 2011.
23. Boyacioglu P, Bevan A, Vickerstaff A. Use of NDT inspection data to improve rail damage prediction models. In: IET Conference Publications. 2018.